THE JOURNAL OF PHYSICAL CHEMISTRY B

ARTICLE

pubs.acs.org/JPCB

Solvent Effects on 3-Keto-1*H*-pyrido[3,2,1-*kl*]phenothiazine Fluorescence in Polar and Protic Solvents

Songqiu Yang,[†,‡] Jianyong Liu,[†] Panwang Zhou,[†] and Guozhong He[†,*]

[†]State Key Laboratory of Molecular Reaction Dynamics, Dalian Institute of Chemical Physics, Chinese Academy of Science, Dalian 116023, P. R. China

[‡]Graduate School of the Chinese Academy of Science, Beijing 100039, P. R. China

Supporting Information

ABSTRACT: Solvent effects on 3-keto-1*H*-pyrido[3,2,1-*kl*]-phenothiazine (PTZ-5) fluorescence in aprotic and protic solvents were investigated using the time-dependent density functional theory method. Enhancement of PTZ-5 fluorescence in the polar aprotic solvent is caused by the decoupling of the two proximity low-lying excited singlet states. In polar protic solvents, aside from the solvent polarity effects, hydrogen-bonding effects are significant to the enhancement of fluorescence. Hydrogen bonds confine C−H out-of-plane bending and severely decouple the two low-lying excited singlet states, greatly decreasing nonradiative decay. The excited state intermolecular proton transfer model is considered a quenching reaction for excited PTZ-5; however, it is uncompetitive in excited-state dynamics.

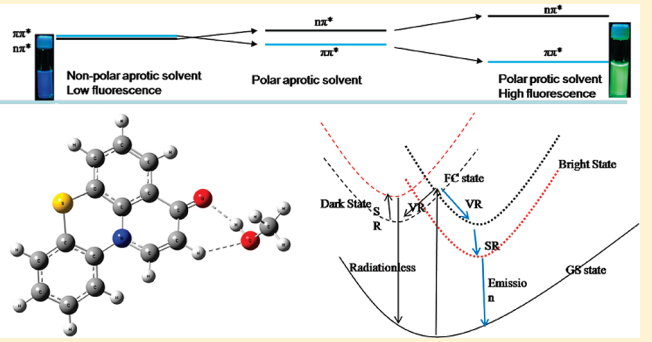

INTRODUCTION

The photophysical and photochemical properties of fluorophores are always affected by solvents.[1−26] These include solvent polarity, viscosity, temperature, and specific solvent and fluorophore interaction. There are two kinds of solvent effects: the general and the specific solvent effects.[1,2] General solvent effects are due to the interactions of the fluorophore dipole with its environment. Solvent polarity is a major factor of general solvent effects. For example, an internal charge-transfer (ICT) state was formed for coumarin-151 (C151) in a polar solvent. Compared with the local excited (LE) state, the ICT state has a smaller nonradiative decay rate (k_{nr}). Thus, the fluorescence of C151 in high-polarity solvents enhanced with the decrease of k_{nr}.[3] In contrast to C151, the ICT state of neutral red has a smaller radiative decay rate (k_r) compared with its LE state. Therefore, the fluorescence quantum yield of neutral red decreased in high-polarity solvents.[4] Specific solvent effects, which are produced by interactions between the fluorophore and neighboring solvent molecules, are more complex than general solvent effects. The fluorescence properties of C151 and neutral red in protic solvents are also affected by specific solvent effects.[3,4] Excited-state proton transfer (ESPT) is considered a very important reaction in the excited-state dynamics of fluorophore.[5−11] Electron transfer between the solute and the solvent also affects the photophysical and photochemical properties of fluorophores.[14]

Actually, the solvent effects on the excited-state dynamics of fluorophores are essential to its photophysical and photochemical properties. Investigating solvent effects on excited-state dynamics helps one to understand the fluorescence properties of fluorophores. Numerous theoretic efforts have been made to describe the excited-state dynamics of fluorophores in different circumstances.[11−13,27−33] The energy gap law is well established.[27] Lim et al. explored a "proximity effect" model to understand the photophysical properties of nitrogen-hytero cyclic or aromatic carbonyl compounds.[12,13] Zgierski et al. found a biradical radiationless decay channel in natural bases.[29−32]

Recently, Han et al. reported some environment-sensitive phenothiazine dyes.[15] Among these (Figure1) are 3-keto-1*H*-pyrido[3,2,1-*kl*]phenothiazine (PTZ-5) and 2,3-dihydro-3-keto-1*H*-pyrido[3,2,1-*kl*]phenothiazine (PTZ-4), both of which show interesting photophysical properties. In protic solvents, PTZ-5 has shown significantly higher fluorescence quantum yields than in aprotic solvents, whereas PTZ-4 was quenched entirely. However, the effects of solvent properties on the fluorescence properties of these two dyes remain unclear.

This paper focuses on the solvent effects on PTZ-5 fluorescence properties. PTZ-4 was also investigated as a comparison. The time-dependent density functional theory (TD-DFT) method was used to investigate the electronic states of PTZ-5 and PTZ-4. The general solvent effects on the fluorescence properties of PTZ-5 and PTZ-4 in several solvents are discussed. Subsequently, the hydrogen-bonding effects on PTZ-5 fluorescence properties are also discussed.

Received: May 12, 2011
Revised: July 26, 2011
Published: August 01, 2011

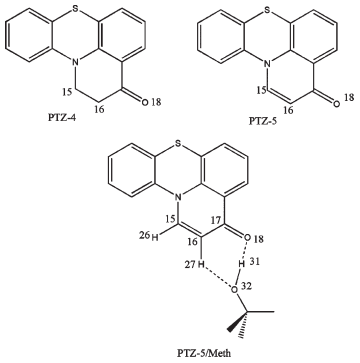

Figure 1. The chemical structures of PTZ-4, PTZ-5, and PTZ-5/Meth complexes.

COMPUTATIONAL METHOD

Calculations were performed using Gaussian 09 programs.[34] The equilibrium geometries of the ground state were optimized using density functional theory (DFT) method. The vertical excited energies were calculated at optimized geometries using the TD-DFT method. TD-DFT was also used to optimize the equilibrium geometries of the excited states. The calculations considered the solvent effects to be performed in the presence of a solvent by placing the solute in a cavity within the solvent reaction field (SCRF). The polarizable continuum model using the integral equation formalism variant (IEF-PCM) is used in SCRF. The B3LYP functional and the 6-31G (d) basis set are used for all calculations.

The potential energy profiles of some states were checked with CC2 type calculations for better discussion.[35] These calculations were carried out with the TURBOMOLE program suite,[36] making use of the resolution-of-the-identity approximation for the evaluation of the electron-repulsion integrals.[37] The TZVP basis set has been employed.[38,39]

RESULTS AND DISCUSSION

Relationship between Fluorescence of the Dyes and Solvent Polarity. The photophysical properties of PTZ-5 and PTZ-4 have been reported previously.[15] The properties are recalled here for a clearer discussion. PTZ-5 and PTZ-4 have similar structures except for the $C_{15}-C_{16}$ bond (Figure 1). Their photophysical properties are very different in solution. Figure 2 shows the fluorescence quantum yields of PTZ-4 and PTZ-5 in solution plotted against the solvent polarity parameters (π^*).[40,41]

For PTZ-4 (Figure 2a), the changes in solvent polarity show no regular effects on fluorescence quantum yields. Figure 2b shows that the fluorescence quantum yields of PTZ-5 are distinctly divided into two regions. One region is associated with aprotic solvents, where the fluorescence quantum yields increase linearly with the increase in solvent polarity. The other region is associated with protic solvents, in which the fluorescence quantum yields behave similarly to those in the aprotic solvent region. Furthermore, the fluorescence quantum yields of PTZ-5 in the protic solvent region are about 5 times larger than those in the aprotic solvent region, indicating special solvent effects on PTZ-5 when in protic solvents. These special solvent effects are expected to be essential to the strongly enhanced fluorescence of PTZ-5 in protic solvents.

Dark State and Bright State. The vertical excited energies of PTZ-5 and PTZ-4 at each ground state (GS) optimized geometries are calculated by TD-DFT (Table 1). These calculated results agree with the experimental absorption spectroscopy.[15] Figure 3 shows the relevant molecular orbitals (MOs) of PTZ-5; Figure S1 (Supporting Information) shows the relevant MOs of PTZ-4.

According to the relevant MOs and Franck−Condon factor, f, the two low-lying excited singlet states of PTZ-5 at the Franck−Condon (FC) region are mixing $n\pi^*$ and $\pi\pi^*$ states. The $n\pi^*$ state is a dark (nonradiative) state, and the $\pi\pi^*$ state is a bright (radiative) state. The optimized geometries of $n\pi^*$ and $\pi\pi^*$ states are obtained by TD-DFT; the Cartesian coordinates of GS, $n\pi^*$, and $\pi\pi^*$ optimized geometries are presented in the Supporting Information. The calculated vertical excited energies of the $n\pi^*$ and $\pi\pi^*$ states at each optimized geometry are also shown in Table 1. The emission peak of PTZ-5 in *n*-hexane is identical to the vertical excited energy of optimized $\pi\pi^*$ state (in vacuum). Figure 4 shows the potential-energy profiles of GS, the first singlet state (S_1), and the second singlet state (S_2) along the linearly interpolated transit path between the GS-optimized geometry and the $n\pi^*$-optimized geometry. The potential-energy profiles of GS, S_1, and S_2 along the linearly interpolated transit path between the GS-optimized geometry and the $\pi\pi^*$-optimized geometry are also shown in Figure 4. There is a conical intersection between the $n\pi^*$ and the $\pi\pi^*$ state around the FC state.

The initial excited-state populations will be divided into two paths from the FC state upon excitation. The populations relax to the $\pi\pi^*$ state is a radiative decay path, whereas the $n\pi^*$ state is a nonradiative decay path. As reported by Han et al.,[15] the fluorescence radiative decay rate constants, k_r, of PTZ-5 are almost the same in all solvents, but the nonradiative decay constants, k_{nr}, decrease severely from protic solvents to aprotic solvents. According to the discussion on C151 and neutral red,[3,4] it is reasonable to suppose that the emission state of PTZ-5 is always $\pi\pi^*$ in all solvents and that the fluorescence quantum yields are modulated by changing the nonradiative decay rate such as C151.

Solvent Polarity Effects on S_1 and S_2 Separation. The quantitative description of the general solvent effects on fluorescence quantum yield is still a challenge in photophysics. Generally, the potential energy surfaces of the excited state will be changed by polar solvents.[1,2,13] The potential energy surface of the $n\pi^*$ state increases, whereas that of the $\pi\pi^*$ state decreases with the increase in the solvent polarity. These changes in potential energy surfaces of fluorophores in the solvent are essential to modulate fluorescence properties. The "energy gap" theory argues that a larger separation between two states implies a smaller coupling.[27] Lim et al. found that the out-of-plane bending couples of the close-lying $n\pi^*$ and $\pi\pi^*$ states and the fluorescence of some fluorophores can be enhanced by polar solvents through decoupling of the two low-lying states.[12,13]

The polarizable continuum model using IEF-PCM was considered to calculate solvent effects on the GS-optimized geometries. The vertical excited energies calculated at GS-optimized geometries considered solvent effects, the results of which are shown in Table 2. The energy levels of the $n\pi^*$ and $\pi\pi^*$ states are separated when solvent effects are considered in calculations. The $\pi\pi^*$ state is lower than the $n\pi^*$ state in polar solvents. The energy separation (ΔE (S_2-S_1)) increases with the increase in the solvent polarity. The S_1 state shows a few red shifts, whereas the S_2 state shows a few blue shifts. As expected, a larger Storks'

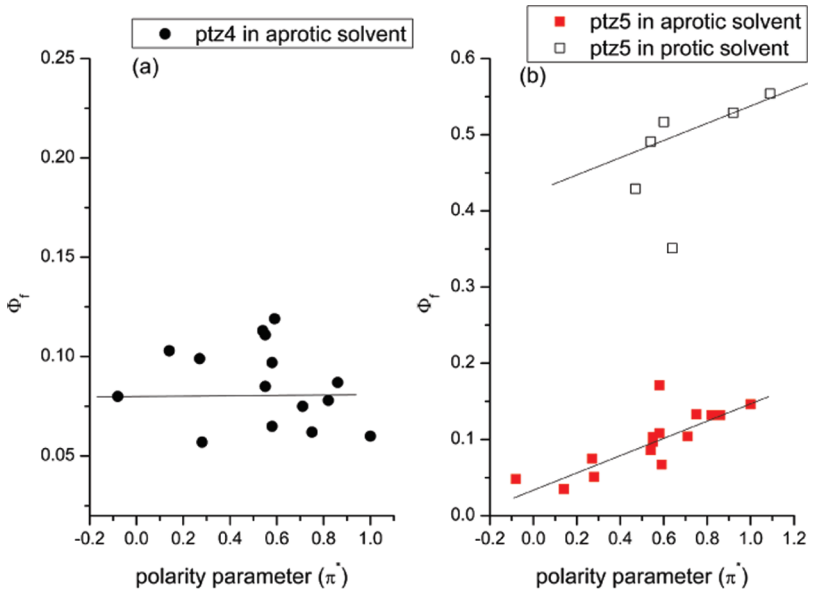

Figure 2. The fluorescence quantum yields of PTZ-4 and PTZ-5 plotted against the solvent polarity parameter π^*. Details of experimental quantum yield results are from ref 15; solvent polarity parameters are cited from refs 40 and 41.

Table 1. Vertical Excited Energies of PTZ-4 and PTZ-5 at Their Optimized Ground State Geometries Calculated at the TD-DFT/B3LYP/6-31G(d) level[a]

geometry	S_1/eV	S_2/eV	ΔE ($S_2 - S_1$)/eV
PTZ-4 GS	3.0457 (3.1548)[b]	3.6882	0.6425
	f = 0.0597	f = 0.0003	
	HOMO → LUMO (100%)	HOMO-2 → LUMO (100%)	
PTZ-5 GS	3.5613 (3.3968)[b]	3.6361	0.0748
	f = 0.0749	f = 0.0800	
	HOMO → LUMO (52%)	HOMO → LUMO (9%)	
	HOMO-1 → LUMO (48%)	HOMO-1 → LUMO (46%)	
		HOMO-2 → LUMO (45%)	
PTZ-5 $n\pi^*$	2.9106	3.3697	
	f = 0.0008	f = 0.1523	
	HOMO → LUMO (2%)	HOMO → LUMO (92%)	
	HOMO-1 → LUMO (98%)	HOMO-2 → LUMO (8%)	
PTZ-5 $\pi\pi^*$	2.8932 (2.8968)[b]	3.3447	
	f = 0.1285	f = 0.0004	
	HOMO → LUMO (100%)	HOMO-2 → LUMO (100%)	

[a] The vertical excited energies of the $n\pi^*$ and $\pi\pi^*$ states are calculated at each optimized geometry. The relevant MOs and their contributions of each transition are listed, as well. f is the oscillator strength. [b] The data in parentheses are experimental results which are cited from ref 15; the solvent is *n*-hexane.

shift was found in the more polar solvent.[15] Subsequently, the dark state equilibrium populations will be decreased by increasing the solvent polarity; the bright state populations will be increased so that fluorescence is enhanced. This is in agreement with the results in Figure 2b showing that the quantum yields increase with the increase in solvent polarity.

Hydrogen-Bond Effects on S_1 and S_2 Separation. The vertical excited energies of PTZ-5 and monomethanol complex (PTZ-5/Meth, Figure 1) at their optimized ground state geometries are listed in Table 2. The IEF-PCM model was used in the SCRF method. The energy separations between S_1 and S_2 for PTZ-5 in both THF and methanol (no hydrogen-bonding complex) are similar because the solvent polarity effects on the potential energy surface of PTZ-5 in both THF and methanol are almost the same. However, the formation of a hydrogen-bonding complex dramatically changes the potential energy surfaces of the excited states. The calculated energy separation of S_1 and S_2 is 0.47 eV for PTZ-5/Meth in methanol, much greater than that for PTZ-5 in methanol (no hydrogen-bonding complex, ΔE ($S_2 - S_1$) = 0.28 eV) and for PTZ-5 in vacuum (ΔE ($S_2 - S_1$) = 0.08 eV). A large separation therefore severely decouples the two low-lying excited states for PTZ-5 in methanol.

Effect of S_1 and S_2 Separation on Fluorescence. According to the "proximity effect" theory, a larger energy gap between the proximity $n\pi^*$ and $\pi\pi^*$ states will induce higher fluorescence quantum yields for some fluorophores.[12,13] In the cases we

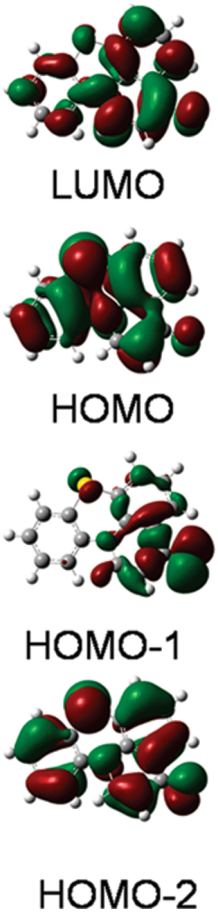

Figure 3. The relevant molecular orbitals of PTZ-5 calculated at ground state optimized geometry.

discussed here, PTZ-5 possesses two proximity low-lying singlet excited states: $n\pi^*$ and $\pi\pi^*$. The separation between these two states increases with the increase in the solvent polarity. A large separation decouples the two low-lying excited states. Subsequently, the fluorescence quantum yields increases in polar solvents. For PTZ-5 in a protic solvent, a large separation is obtained by the formation of a hydrogen-bonding complex, which decouples $n\pi^*$ and $\pi\pi^*$ states then induces enhanced fluorescence.

However, the fluorescence properties of PTZ-4 in an aprotic solvent are not the same as PTZ-5 (Figure 2a). The fluorescence of PTZ-4 shows no regular changes with the increase in the solvent polarity. This is attributed to the large separation between the two low-lying S_1 ($\pi\pi^*$) and S_2 ($n\pi^*$) states of PTZ-4, where there is no coupling between S_1 and S_2 at all [Table 1, ΔE (S_2-S_1) = 0.64 eV].

The Role of $-H_{26}C_{15}=C_{16}H_{27}-$ in Excited-State Dynamics. Literature has shown that the torsion of the $-HC=CH-$ dihedral angle can induce conical intersection (CI) between S_1 and GS or between S_1 and S_2. This torsion is a major decay path of nonradiation for some natural bases and their derivatives.[28−33] As mentioned previously, the fluorescence of PTZ-4 was quenched entirely, but that of PTZ-5 was strongly enhanced in the protic solvent.[15] The difference in structure between PTZ-5 and PTZ-4 is the $C_{15}-C_{16}$ bond. PTZ-5 has a similar structure with uracil at $N-C_{15}=C_{16}-C_{17}=O_{18}$. It is therefore reasonable to assume that the deformation of the $HC_{15}=C_{16}H$ double bond in PTZ-5 should be an important nonradiative decay path. The

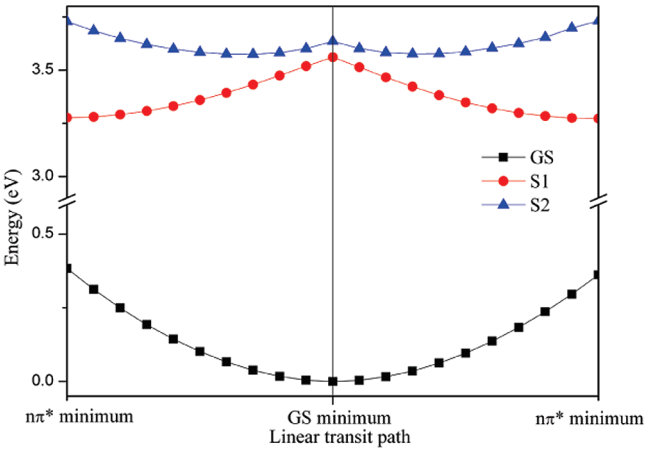

Figure 4. Potential-energy profiles of GS, S_1, and S_2 for the linearly interpolated transit path between GS and $n\pi^*$, GS and $\pi\pi^*$ optimized geometries for PTZ-5. The energy of GS-optimized geometry was set to zero.

vertical excited energies were calculated at the redundant GS-optimized geometries by changing the dihedral angle of $H_{26}C_{15}=C_{16}H_{27}$. The potential energy profiles of GS and the $n\pi^*$ and $\pi\pi^*$ states are shown in Figure 5 (the excited states are actually the mixes between $n\pi^*$ and $\pi\pi^*$; these are identified by the relevant MOs). A conical intersection is found between $n\pi^*$ and $\pi\pi^*$ located at approximately the FC state. It confirms that the out-of-plane bending of $H_{26}C_{15}=C_{16}H_{27}$ is essential in the excited-state dynamics of PTZ-5, which can induce nonradiative decay from the FC state to dark state as well as internal conversion decay between the dark and bright states.

Hydrogen-Bond Confines Out-of-Bending. Considering the formation of hydrogen bonds between PTZ-5 and methanol, a six-atom cycle is formed (Figure 1). In addition to the hydrogen bond formed between $-C_{17}=O_{18}\cdots H_{31}-$, a very weak hydrogen bond is also formed between $-C_{16}-H_{27}\cdots O_{32}-$. The latter hydrogen bond is considered to confine the out-of-plane bending of $C_{16}-H_{27}$. This confined effect hinders nonradiative decay from the FC state to the dark state as well as internal conversion between S_1 and S_2. Therefore, hydrogen-bonding decreases fluorescence quenching. Zgierski et al. found that the formation of a hydrogen bond between $-C_5-H\cdots O-$ in N^4-acetylcytosine increases the fluorescence quantum yields by confining the out-of-plane bending of $-C_5-H$. In N^4-acetylcytosine, the hydrogen bond is an intramolecular bond; however, for PTZ-5 in a protic solvent, the hydrogen bond is formed between the solute and the solvent molecules. Nonetheless, both intra- and intermolecular hydrogen bonds confine the out-of-plane bending of C−H. This prohibitive effect is the explanation for the difference in the fluorescence quantum yield of PTZ-5 in protic and aprotic environments.

Excited-State Proton Transfer Process. Generally, the excited-state proton transfer (ESPT) is considered a quenching mechanism rather than an enhancing mechanism for fluorophore in a protic solvent.[7−11] To investigate ESPT, the potential energy profiles of GS, S_1, and S_2 were calculated at each redundant GS-optimized geometry along the change distance of O_{18} and H_{31}. Figure S3 of the Supporting Information shows that the initial populations at the FC state can decay to the ground state through ESPT. A small barrier (0.15 eV) should be conquered in this decay path. This barrier is surprisingly low and would make

Table 2. Vertical Excited Energies of PTZ-4 and PTZ-5 at Their Optimized Ground State Geometries Calculated at the TD-DFT/B3-LYP/6-31G(d) Level[a]

molecule	solvent	parameter π^*	S_1/eV	S_1 (exp) /eV	S_2/eV	ΔE ($S_2 - S_1$)/eV
PTZ-5	*n*-hexane	−0.08	3.5342	3.3968	3.6721	0.1379
PTZ-5	CCl_4	0.28	3.5254	3.3419	3.6854	0.1600
PTZ-5	THF	0.58	3.5081	3.3692	3.7533	0.2452
PTZ-5	meth	0.60	3.5035	3.2975	3.7835	0.2803
PTZ-5	acetonitrile	0.75	3.5018	3.3600	3.7848	0.2830
PTZ-5	DMSO	1.00	3.4958	3.3151	3.7867	0.2909
PTZ5/Meth	meth	0.60	3.4120	3.2975	3.8862	0.4742

[a] The IEF-PCM model is considered in SCRF to deal with solvent effects. Experimental (exp) data were obtained from ref 15.

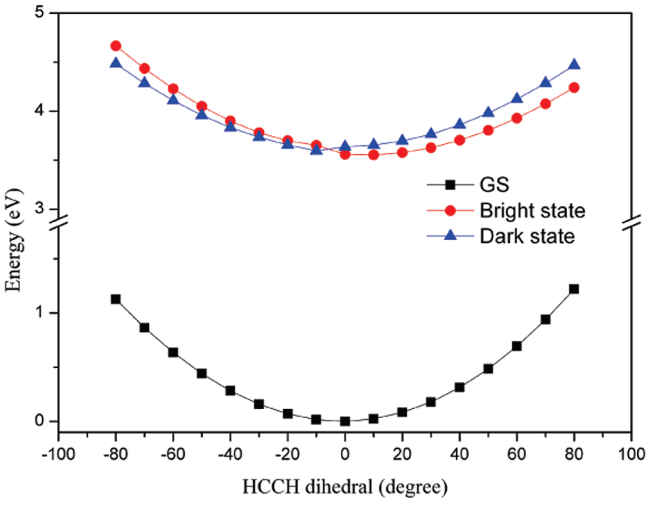

Figure 5. Potential-energy profiles of the bright state ($\pi\pi^*$) and the dark state ($n\pi^*$) as a function of $H_{26}C_{15}{=}C_{16}H_{27}$ dihedral angle. The energy of GS optimized geometry was set to zero.

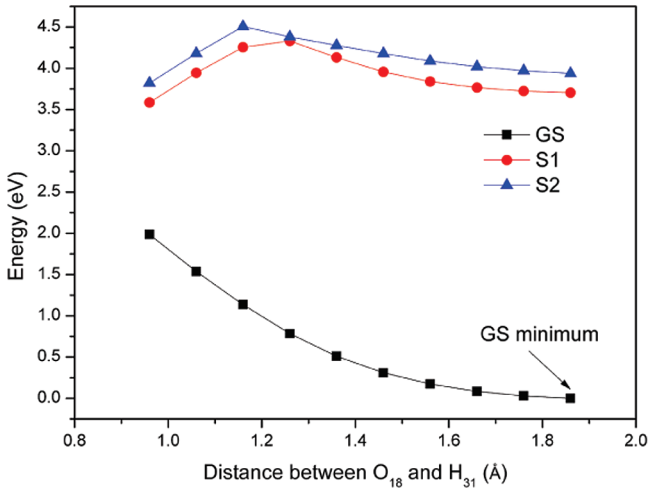

Figure 6. Potential-energy profiles of the two low-lying excited states and GS as a function of distance between O_{18} and H_{31} calculated by the CC2 method. The energy of the GS-optimized geometry was set to zero.

ESPT an efficient channel for radiationless decay. The TD-B3LYP calculations may result in artificially low energy. To check this barrier, the potential energy profiles of GS, S_1, and S_2 were calculated by the CC2 method. The results are shown in Figure 6. There is a barrier, 0.63 eV, in the ESPT path so that ESPT is still a quenching reaction for excited PTZ-5, but a barrier should be conquered.

Han et al. reported interesting fluorescence properties of PTZ-5 in the acidic solution.[15] At a pH value below 3, the fluorescence decreases sharply with the decrease in the pH value. This indicates that a high H^+ concentration would be a fluorescence quenching factor, not an enhancing factor. This is consistent with the current ESPT results. However, ESPT should be unimportant for PTZ-5 in protic solvents because enhanced fluorescence was obtained in the experiment; this may be due to the barrier in the ESPT path.

The Excited-State Dynamics Scheme of PTZ-5. Schematic representation of the excited-state dynamics of PTZ-5 in solution is shown in Figure 7. There are three decay paths from the initial FC state. The populations at the FC state will be relaxed to the dark and bright states by vibrational relaxation (VR) or relaxed to the GS state through ESPT. However, ESPT is unimportant in excited-state dynamics and is therefore not shown in Figure 7.

The dark ($n\pi^*$) and the bright ($\pi\pi^*$) states are coupled strongly to each other, and an equilibration is established between them. In a polar solvent, the bright state is relatively lower than the dark state. This is beneficial for the excited molecules to populate into the bright state and for the decoupling of the two low-lying excited states. Therefore, a higher barrier and a slower internal conversion process from the FC and the bright state to the dark state will be obtained by increasing the solvent polarity. As a result, the nonradiative decay rate decreases.

Aside from the solvent polarity effects, three other effects on the fluorescence properties of PTZ-5 in a protic solvent were detected. The nonradiative decay from the FC to the dark state may be suppressed by the two effects. One is by confining the out-of-plane bending of $C_{16}{-}H_{27}$ through hydrogen-bonding between O_{32} and H_{27}; the other is changing the potential energy surface of PTZ-5 through the formation of a hydrogen bonding complex. The general solvent effects of THF and methanol on potential energy surfaces will be similar because of similar polarity; however, the potential energy surfaces were changed dramatically by hydrogen-bonding. A large separation between the dark and the bright states will be obtained for PTZ-5 in a protic solvent. This will decouple the two low-lying excited singlet states severely, then reduce the decay from the FC to the dark state and change the equilibrium populations on the bright and the dark states. The third effect is ESPT, which causes fluorescence quenching. ESPT needs to conquer a barrier to decay the excited populations. However, decay from the FC state to the bright state optimized geometry is a nonbarrier process. It is reasonable to

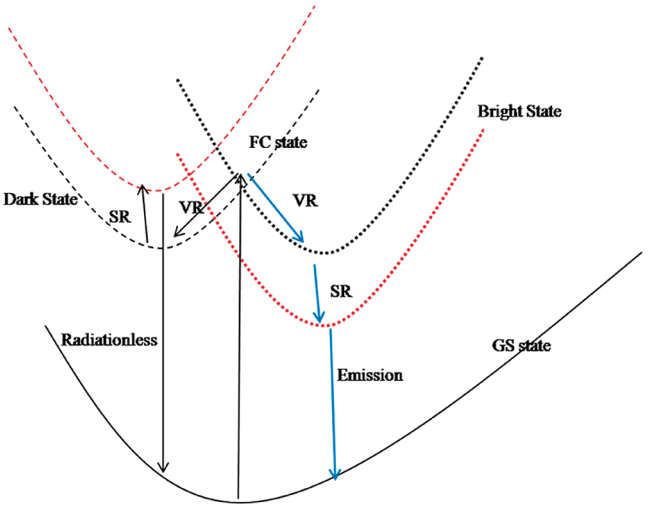

Figure 7. Schematic representation of the excited-state dynamics of PTZ-5. FC, Franck−Condon; VR, vibrational relaxation; SR, solvent relaxation; GS, ground state.

suppose that the ESPT mechanism competes with the other two but is insignificant for PTZ-5 in a protic solvent.

CONCLUSION

DFT and TD-DFT methods were used to study the electronic states of PTZ-5 and PTZ-4. Their respective fluorescence properties in different solvents were also discussed. A distinct scheme and a qualitative conclusion to understand the fluorescence properties of these two dyes were established. The two low-lying excited singlet states are the $n\pi^*$ and $\pi\pi^*$ states for both PTZ-4 and PTZ-5. A large separation of the two low-lying excited states for PTZ-4 decouples these two states entirely. Therefore, a change in solvent polarity has no effect on the fluorescence quantum yield of PTZ-4. However, PTZ-5 has very close $n\pi^*$ and $\pi\pi^*$ states that are coupled strongly. Increasing the polarity of the solvent enhances fluorescence for PTZ-5 through the decoupling of the two proximity excited singlet states. The formation of a hydrogen-bonding complex for PTZ-5 in a protic solvent not only confines the out-of-plane bending of C16−H27 but also increases the separation of $n\pi^*$ and $\pi\pi^*$. These strongly enhance the fluorescence of PTZ-5 in a protic solvent. The ESPT process is a quenching reaction for excited PTZ-5 in a protic solvent but is uncompetitive in excited-state dynamics.

ASSOCIATED CONTENT

Supporting Information. Text giving the relevant molecular orbitals of PTZ-4 calculated at GS optimized geometry; the relevant molecular orbitals of PTZ-5 calculated at optimized GS, $n\pi^*$, and $\pi\pi^*$ states; potential-energy profiles of the two low-lying excited states and GS as a function of distance between O_{18} and H_{31} calculated at TD-B3LYP/6-31G(d) level; Cartesian geometries of the optimized ground, dark, and bright states of PTZ-5. This material is available free of charge via the Internet at http://pubs.acs.org.

AUTHOR INFORMATION

Corresponding Author
*E-mail: gzhe@dicp.ac.cn.

ACKNOWLEDGMENT

We thank Prof. Dr. Jianzhang Zhao for helpful discussions. This work was supported by NSFC (No.20973168).

REFERENCES

(1) Lakowicz, J. R. *Principles of Fluorescence Spectroscopy*, 3rd ed.; Springer Science + Business Media, LLC: New York, 2006.
(2) Klymchenko, A. S.; Demchenko, A. R. *Fluoresc. Spectrosc.* **2008**, *450*, 37–58.
(3) Nad, S.; Pal, H. *J. Phys. Chem. A* **2001**, *105*, 1097–1106.
(4) Singh, M. K.; Pal, H.; Bhasikuttan, A. C.; Sapre, A. V. *Photochem. Photobiol.* **1998**, *68*, 32–38.
(5) Shemesh, D.; Sobolewski, A. L.; Domcke, W. *Phys. Chem. Chem. Phys.* **2010**, *12*, 4899–4905.
(6) Qian, J.; Brouwer, A. M. *Phys. Chem. Chem. Phys.* **2010**, *12*, 12562–12569.
(7) Zhao, G. J.; Northrop, B. H.; Han, K. L.; Stang, P. J. *J. Phys. Chem. A* **2010**, *114*, 9007–9013.
(8) Ke-Li Han, G.-J. Z., *Hydrogen Bonding and Transfer in the Excited State*; John Wiley & Sons, Ltd: New York, 2010; Vol. 1−2.
(9) Zhao, G. J.; Han, K. L. *Biophys. J.* **2008**, *94*, 38–46.
(10) Aquino, A. J. A.; Lischka, H.; Hattig, C. *J. Phys. Chem. A* **2005**, *109*, 3201–3208.
(11) Sinicropi, A.; Nau, W. M.; Olivucci, M. *Photochem. Photobiol. Sci.* **2002**, *1*, 537–546.
(12) Wassam, W. A.; Lim, E. C. *J. Chem. Phys.* **1978**, *68*, 433–454.
(13) Lim, E. C. *J. Phys. Chem.* **1986**, *90*, 6770–6777.
(14) Lemmetyinen, H.; Tkachenko, N. V.; Efimov, A.; Niemi, M. *Phys. Chem. Chem. Phys.* **2011**, *13*, 397–412.
(15) Han, F.; Chi, L.; Wu, W.; Liang, X.; Fu, M.; Zhao, J. *J. Photochem. Photobiol., A* **2008**, *196*, 10–23.
(16) Sumitani, M.; Nakashima, N.; Yoshihara, K.; Nagakura, S. *Chem. Phys. Lett.* **1977**, *51*, 183–185.
(17) Lakowicz, J. R.; Balter, A. *Photochem. Photobiol.* **1982**, *36*, 125–132.
(18) de Melo, J. S. S.; Becker, R. S.; Macanita, A. L. *J. Phys. Chem.* **1994**, *98*, 6054–6058.
(19) de Melo, J. S.; Becker, R. S.; Elisei, F.; Macanita, A. L. *J. Chem. Phys.* **1997**, *107*, 6062–6069.
(20) Haidekker, M. A.; Ling, T. T.; Anglo, M.; Stevens, H. Y.; Frangos, J. A.; Theodorakis, E. A. *Chem. Biol.* **2001**, *8*, 123–131.
(21) Cave, R. J.; Burke, K.; Castner, E. W. *J. Phys. Chem. A* **2002**, *106*, 9294–9305.
(22) Uchiyama, S.; Takehira, K.; Yoshihara, T.; Tobita, S.; Ohwada, T. *Org. Lett.* **2006**, *8*, 5869–5872.
(23) Zhao, G. J.; Han, K. L. *J. Phys. Chem. A* **2007**, *111*, 9218–9223.
(24) Gota, C.; Uchiyama, S.; Yoshihara, T.; Tobita, S.; Ohwada, T. *J. Phys. Chem. B* **2008**, *112*, 2829–2836.
(25) Yu, F.; Li, P.; Li, G.; Zhao, G.; Chu, T.; Han, K. *J. Am. Chem. Soc.* **2011**, *133*, 11030.
(26) Peng, X. J.; Wu, Y. K.; Fan, J. L.; Tian, M. Z.; Han, K. L. *J. Org. Chem.* **2005**, *70*, 10524.
(27) Caspar, J. V.; Meyer, T. J. *J. Phys. Chem.* **1983**, *87*, 952–957.
(28) Matsika, S. *J. Phys. Chem. A* **2004**, *108*, 7584–7590.
(29) Zgierski, M. Z.; Patchkovskii, S.; Fujiwara, T.; Lim, E. C. *J. Phys. Chem. A* **2005**, *109*, 9384–9387.
(30) Zgierski, M. Z.; Patchkovskii, S.; Lim, E. C. *J. Chem. Phys.* **2005**, 123.
(31) Zgierski, M. Z.; Patchkovskii, S.; Fujiwara, T.; Lim, E. C. *Chem. Phys. Lett.* **2007**, *440*, 145–149.
(32) Zgierski, M. Z.; Patchkovskii, S.; Lim, E. C. *Can. J. Chem.* **2007**, *85*, 124–134.
(33) Delchev, V. B.; Sobolewski, A. L.; Domcke, W. *Phys. Chem. Chem. Phys.* **2010**, *12*, 5007–5015.
(34) Frisch, M. J.; Trucks, G. W.; Schlegel, H. B.; Scuseria, G. E.; Robb, M. A.; Cheeseman, J. R.; Scalmani, G.; Barone, V.; Mennucci, B.;

Petersson, G. A.; Nakatsuji, H.; Caricato, M.; Li, X.; Hratchian, H. P.; Izmaylov, A. F.; Bloino, J.; Zheng, G.; Sonnenberg, J. L.; Hada, M.; Ehara, M.; Toyota, K.; Fukuda, R.; Hasegawa, J.; Ishida, M.; Nakajima, T.; Honda, Y.; Kitao, O.; Nakai, H.; Vreven, T.; Montgomery, J. A., Jr.; Peralta, J. E.; Ogliaro, F.; Bearpark, M.; Heyd, J. J.; Brothers, E.; Kudin, K. N.; Staroverov, V. N.; Kobayashi, R.; Normand, J.; Raghavachari, K.; Rendell, A.; Burant, J. C.; Iyengar, S. S.; Tomasi, J.; Cossi, M.; Rega, N.; Millam, N. J.; Klene, M.; Knox, J. E.; Cross, J. B.; Bakken, V.; Adamo, C.; Jaramillo, J.; Gomperts, R.; Stratmann, R. E.; Yazyev, O.; Austin, A. J.; Cammi, R.; Pomelli, C.; Ochterski, J. W.; Martin, R. L.; Morokuma, K.; Zakrzewski, V. G.; Voth, G. A.; Salvador, P.; Dannenberg, J. J.; Dapprich, S.; Daniels, A. D.; Farkas, Ö.; Foresman, J. B.; Ortiz, J. V.; Cioslowski, J.; Fox, D. J. *Gaussian 09*, Revision A.02; Gaussian, Inc.: Wallingford, CT, 2009.

(35) Christiansen, O.; Koch, H.; Jorgensen, P. *Chem. Phys. Lett.* **1995**, *243*, 409–418.

(36) Ahlrichs, R.; Bar, M.; Haser, M.; Horn, H.; Kolmel, C. *Chem. Phys. Lett.* **1989**, *162*, 165–169.

(37) Weigend, F.; Haser, M. *Theor. Chem. Acc.* **1997**, *97*, 331–340.

(38) Schafer, A.; Huber, C.; Ahlrichs, R. *J. Chem. Phys.* **1994**, *100*, 5829–5835.

(39) Weigend, F.; Haser, M.; Patzelt, H.; Ahlrichs, R. *Chem. Phys. Lett.* **1998**, *294*, 143–152.

(40) Kamlet, M. J.; Abboud, J. L. M.; Abraham, M. H.; Taft, R. W. *J. Org. Chem.* **1983**, *48*, 2877–2887.

(41) Marcus, Y. *Chem. Soc. Rev* **1993**, *22*, 409–416.